

Forward-backward asymmetries of fourth family fermions through the Z' models at linear colliders

V. Ari,^{*} O. Çakır,[†] and V. Çetinkaya[‡]*Department of Physics, Faculty of Sciences, Ankara University, 06100 Tandogan, Ankara, Turkey*

(Received 8 May 2012; published 11 February 2013)

We investigate the forward-backward asymmetries in the pair production of fourth-family fermions through the new Z' interactions in e^+e^- collisions. A Z' boson with family-universal couplings can contribute to the pair production of fourth-family fermions via the s -channel exchange. Linear colliders provide a clean environment for the physics of the Z' boson in order to measure its couplings precisely. The effects of the Z' boson on the asymmetries are shown to be important in some parameter regions for different Z' models. Among these parameters, the invariant mass distribution $m_{F\bar{F}}$ will be an important measurement to constrain the Z' models. Providing that fourth-family fermions exist in an accessible mass range, a χ^2 analysis can be used to probe the Z' models at linear colliders.

DOI: [10.1103/PhysRevD.87.035013](https://doi.org/10.1103/PhysRevD.87.035013)

PACS numbers: 12.60.-i, 14.60.Hi, 14.70.Pw

1. INTRODUCTION

Even though we observe three families of quarks and leptons in the Standard Model (SM), there could however be a fourth family if their masses and mixings are beyond our present experimental reach. A family extension to the SM fermion families contains the quarks t' and b' , and the charged lepton l' with its associated neutrino ν' . The allowed parameter space for a fourth family is restricted by experimental searches, precision electroweak measurements, and theoretical constraints from the requirements of unitarity and perturbativity.

Recent searches at the Large Hadron Collider (LHC) have considered pair production of the fourth-family quarks. A search by the ATLAS Collaboration in the dilepton final state using 4.7 fb^{-1} of data restricts the masses of t' and b' quarks: $m_{t'} > 656 \text{ GeV}$ at 95% C.L. [1] assuming $t' \rightarrow W^+b$, and $m_{b'} > 670 \text{ GeV}$ at 95% C.L. [2] assuming $b' \rightarrow W^-t$. The CMS Collaboration searched for fourth-generation down-type (up-type) heavy quarks in same-sign dilepton or trilepton events with at least one b -tagged jet, and set a lower mass limit of 611 (570) GeV at 95% C.L. [3,4] assuming a branching fraction of 100% for the decays $b' \rightarrow W^-t$ and $t' \rightarrow W^+b$ at 4.9 fb^{-1} of pp data at $\sqrt{s} = 7 \text{ TeV}$.

From direct production searches at LEP II, there is a lower limit of the order of 100 GeV for the fourth-family charged lepton and unstable neutrino. The precision measurements restrict the mass splitting between the fourth-family leptons $|M_{l'} - M_{\nu'}| \approx 30\text{--}60 \text{ GeV}$ and the fourth-family quarks $|M_{t'} - M_{b'}| \approx 50\text{--}70 \text{ GeV}$ [5,6].

An extra family also affects the phenomenology of the Higgs, leading to changes in the decays $\Gamma(h \rightarrow gg)$ and

$\Gamma(h \rightarrow \gamma\gamma)$. The hints of an SM-like Higgs boson with mass of $\sim 125 \text{ GeV}$ from the LHC [7], also supported by the Tevatron [8], can impose extra constraints beyond the three-family model. The constraints on the fourth-family model can be relaxed if their decays are altered by some new physics effects or if an extended electroweak symmetry breaking exists. For example, a model with two Higgs doublets [9] can be designed to reproduce the hints at $\sim 125 \text{ GeV}$ from the LHC and Tevatron. In this case, quark-sector mass splittings less than m_W are still favored [10].

The fourth-family quarks and leptons could also couple to an extra neutral gauge boson different from the three SM families. A new neutral gauge boson Z' can have family-universal or nonuniversal couplings to fermions. Indirect searches for the Z' boson can also be performed at linear colliders, where the discovery limits are related to the deviations from the SM predictions for the cross sections and asymmetries due to the interference effects between the propagators. A Z' boson with family-universal couplings can contribute to the pair production of fourth-family fermions via the s -channel exchange. Linear colliders provides a clean environment for Z' physics, and can measure the couplings precisely.

In the extensions of the SM with $U(1)_\psi \times U(1)_\chi$ gauge symmetry, the fields Z'_ψ and Z'_χ can be massive and their states can mix; therefore, a relatively lighter mass eigenstate can be written as $Z'(\theta) = Z'_\psi \cos\theta + Z'_\chi \sin\theta$. A set of Z' models have some special names: the sequential Z'_S model has the same coupling to the fermions as that of the Z boson of the SM; the Z'_ψ , Z'_χ , and Z'_η models corresponding to the specific values of the mixing angle θ (0 , $\pi/2$, and $\arctan\sqrt{3/5}$, respectively) in the E_6 model have different couplings to the fermions; the Z'_{B-L} model has the couplings related to the minimal $B-L$ (where B and L are baryon and lepton numbers, respectively) extension of the

*volkan.ari@science.ankara.edu.tr

†ocakir@science.ankara.edu.tr

‡volkan.cetinkaya@science.ankara.edu.tr

SM. Detailed descriptions of the Z' models, as well as other specific references, can be found in Refs. [11–14].

The Tevatron experiments excluded the sequential Z'_S boson with a mass lower than 1 TeV at 95% C.L. [15]. Results of searches for narrow resonances $Z' \rightarrow \ell^+ \ell^-$ have previously been reported by the ATLAS [16] and CMS [17] Collaborations. Recent measurements by the ATLAS and CMS Collaborations based on 5 fb^{-1} of data excludes a Z'_S with a mass lower than 2.22 TeV [18] and 2.33 TeV [19], respectively.

These limits on the Z' boson mass favor high-energy (≥ 1 TeV) collisions for the observation of signals from most of the Z' models. It is also possible that the Z' bosons can be heavy or weak enough to escape beyond the discovery reach expected at the LHC. In this case, only the indirect signatures of Z' exchanges may occur at the high-energy colliders.

Recently, the D0 and CDF Collaborations have measured the forward-backward (FB) asymmetries of the top quark A_{FB}^t at the Tevatron [20,21] in the large $t\bar{t}$ invariant-mass region, while the A_{FB}^b was measured in the Z boson decays at LEP [22]—which differ by about 3σ from the SM expectations—without significantly affecting the well-behaved total cross sections. Several models of new physics have been considered to explain these asymmetries (see Refs. [23–25] and references therein) at hadron colliders.

In this study, we investigate the forward-backward asymmetries A_{FB}^F for pair production of the fourth-family fermions $F_i(t', b', l', \nu')$ within the Z' models at linear collider energies of 1 and 3 TeV. The linear colliders—namely, the International Linear Collider (ILC) described in Refs. [26,27] and the Compact Linear Collider (CLIC) described in Refs. [28,29]—have been designed to meet the baseline requirements for the planned physics programs. The effects of the Z' boson on the asymmetries

of fourth-family fermions at linear colliders are shown to be important in some parameter regions for the sequential model, some special E_6 models, and the $B-L$ model. We will typically consider the mass of the fourth-family charged lepton to be greater than 200 GeV and the masses of the fourth-family quarks to be greater than 600 GeV, which are safely above the direct production bounds.

II. INTERACTIONS WITH FOURTH-FAMILY FERMIONS

The interactions of the fourth-family quarks (Q_i) via neutral gauge bosons (g, γ, Z, Z') and the fourth-family leptons (L_i) via electroweak gauge bosons (γ, Z, Z') can be described by the following Lagrangian. We also include the interactions of fourth-family fermions (F_i) with the three known families of fermions (f_i) through the charged currents (via W^\pm bosons):

$$\begin{aligned} L' = & -g_s \bar{Q}_i T^a \gamma^\mu Q_i G_\mu^a - g_e Q_F \bar{F}_i \gamma^\mu F_i A_\mu \\ & - \frac{g}{2\sqrt{2}} V_{ij} \bar{F}_i \gamma^\mu (1 - \gamma^5) f_j W_\mu \\ & - \frac{g_Z}{2} \bar{F}_i \gamma^\mu (C_V^F - C_A^F \gamma^5) F_i Z_\mu \\ & - \frac{g_{Z'}}{2} \bar{F}_i \gamma^\mu (C_V^{F'} - C_A^{F'} \gamma^5) F_i Z'_\mu + \text{H.c.}, \quad (1) \end{aligned}$$

where $g_s, g_e,$ and g_Z are the strong, electromagnetic, and weak-neutral coupling constants, respectively. The $G_\mu^a, A_\mu, W_\mu,$ and Z_μ are the fields for gluons, photons, and W and Z bosons, respectively. The C_V^F (C_V) and C_A^F (C_A) are vector and axial-vector couplings with the Z' (Z) boson and they are given in Table I.

The decay widths into the heavy-fermion pair $F\bar{F}$ and W^+W^- bosons are given as

TABLE I. The family-independent vector and axial-vector couplings to the new Z' boson predicted by different models.

Down-type quarks		Up-type quarks		Charged leptons		Neutrinos	
C_V'	C_A'	C_V'	C_A'	C_V'	C_A'	C_V'	C_A'
Z'_S							
$-\frac{1}{2} + \frac{2}{3} \sin^2 \theta_W$	$-\frac{1}{2}$	$\frac{1}{2} - \frac{4}{3} \sin^2 \theta_W$	$\frac{1}{2}$	$-\frac{1}{2} + 2 \sin^2 \theta_W$	$-\frac{1}{2}$	$\frac{1}{2}$	$\frac{1}{2}$
Z'_ψ							
0	$\frac{\sqrt{10}}{6} \sin \theta_W$	0	$\frac{\sqrt{10}}{6} \sin \theta_W$	0	$\frac{\sqrt{10}}{6} \sin \theta_W$	$\frac{\sqrt{10}}{12} \sin \theta_W$	$\frac{\sqrt{10}}{12} \sin \theta_W$
Z'_χ							
$\frac{\sqrt{6}}{3} \sin \theta_W$	$-\frac{\sqrt{6}}{6} \sin \theta_W$	0	$\frac{\sqrt{6}}{6} \sin \theta_W$	$-\frac{\sqrt{6}}{3} \sin \theta_W$	$-\frac{\sqrt{6}}{6} \sin \theta_W$	$-\sqrt{6} \sin \theta_W$	$-\sqrt{6} \sin \theta_W$
Z'_η							
$\sin \theta_W$	$\frac{1}{3} \sin \theta_W$	0	$4 \sin \theta_W$	$-\sin \theta_W$	$\frac{1}{3} \sin \theta_W$	$-\frac{1}{3} \sin \theta_W$	$-\frac{1}{3} \sin \theta_W$
Z'_{B-L}							
$\frac{2}{3}$	0	$\frac{2}{3}$	0	-2	0	-1	-1

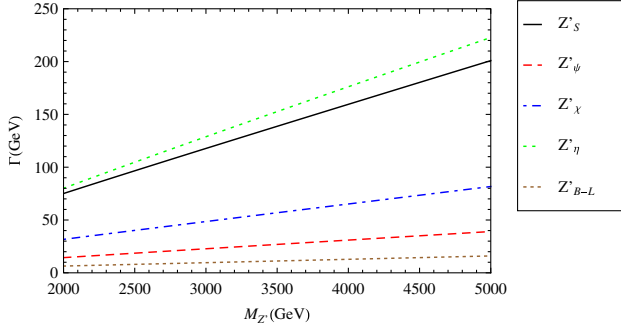


FIG. 1 (color online). The decay widths of the Z' boson predicted by different models in the case of four fermion families.

$$\begin{aligned} \Gamma(Z' \rightarrow F\bar{F}) &= \frac{g_{Z'}^2 N_c}{48\pi M_{Z'}} \sqrt{1 - \frac{4M_F^2}{M_{Z'}^2} [(C_A^{F'})^2 (-4M_F^2 + M_{Z'}^2) + (C_V^{F'})^2 (M_{Z'}^2 + 2M_F^2)]}, \end{aligned} \quad (2)$$

$$\begin{aligned} \Gamma(Z' \rightarrow W^+ W^-) &= \frac{g_W^2 \cos^2 \theta_W \kappa^2}{192\pi M_{Z'} M_W^4} \sqrt{1 - \frac{4M_W^2}{M_{Z'}^2} \left(\frac{M_Z}{M_{Z'}}\right)^4} \\ &\times [M_{Z'}^6 + 16M_W^2 M_{Z'}^4 - 68M_W^4 M_{Z'}^2 - 48M_W^6], \end{aligned} \quad (3)$$

where N_c is the color factor (3 for quarks and 1 for leptons), and $g_{Z'}$ is the coupling constant for the Z' boson. The M_Z , $M_{Z'}$, and M_W are the masses for the Z , Z' , and W bosons, respectively. M_F is the mass of the heavy fermion. The mixing term between the Z' and Z bosons is assumed to be of the order of $M_Z^2/M_{Z'}^2$; hence, a mixing factor κ scales this extension, depending on the specific Z' models. In the sequential model the factor κ is chosen to be unity, which is a reference for the purpose of comparison. In Fig. 1 we present the decay width of the Z' boson versus the mass $M_{Z'}$ in the case of four fermion families. As can be seen from Fig. 1, the total decay width Γ for the Z'_S , Z'_ψ , Z'_χ , Z'_η , and Z'_{B-L} models are about 117, 23, 48, 129, and 10 GeV at a mass value of $M_{Z'} = 3000$ GeV, respectively.

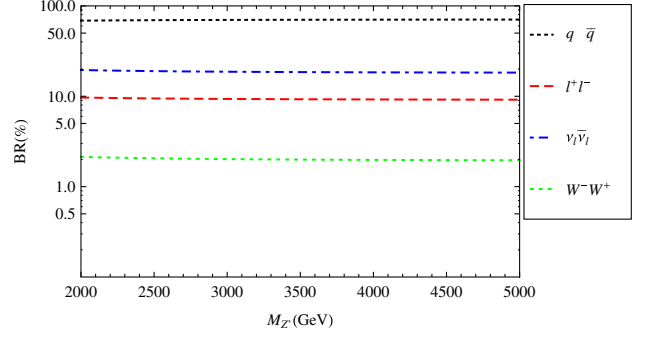


FIG. 2 (color online). The branching ratios of the sequential Z' boson into different final states depending on the mass.

For the sequential Z' model, the branching ratios of all fermionic modes are not very sensitive to $M_{Z'}$, leading to the fractions of about 0.7, 0.2, 0.1, and 0.02 for $Z' \rightarrow q\bar{q}$, $Z' \rightarrow \nu\bar{\nu}$, $Z' \rightarrow l^+ l^-$, and $Z' \rightarrow W^+ W^-$, respectively. In Fig. 2, the $q\bar{q}$ mode includes the quarks from all four families, and the $l^+ l^-$ ($\nu\bar{\nu}$) mode includes the charged leptons (neutrinos) of all four families.

III. CROSS SECTIONS

Using the interaction Lagrangian (1) we calculate the differential cross section for the pair production of fourth-family quarks and leptons in the collisions of e^+ and e^- beams. The analytical expressions for the differential cross section are given in the Appendix. We calculate the cross section for the pair production of fourth-family quarks (leptons), taking their masses in the interval 600–1000 (200–800) GeV. Table II shows the production cross sections without the Z' contribution at ILC and CLIC energies. The ILC, with $\sqrt{s} = 1$ TeV, has the potential, up to the kinematical range ($m_{l',\nu'} \leq 500$ GeV), for the production cross section of fourth-family lepton pairs. However, the CLIC, with $\sqrt{s} = 3$ TeV, extends the mass range for the fourth-family fermions. In order to see the contributions from Z' -boson exchange and its interference we also calculate the cross sections assuming the reference mass values $M_{b'} = 650$ GeV and $M_{\nu'} = 100$ GeV, with the constraints $M_{b'} - M_{l'} \approx 50$ GeV and $M_{l'} - M_{\nu'} \approx 100$ GeV. The cross sections for $l'l'$ and $\nu'\nu'$ pair production

TABLE II. The cross sections (in fb) for the fourth-family pair production processes (without Z') at CLIC with $\sqrt{s} = 3$ TeV. The numbers in parentheses show the results for ILC with $\sqrt{s} = 1$ TeV.

Mass (GeV)	$e^+ e^- \rightarrow \nu' \bar{\nu}'$	$e^+ e^- \rightarrow l'^+ l'^-$	Mass (GeV)	$e^+ e^- \rightarrow b' \bar{b}'$	$e^+ e^- \rightarrow t' \bar{t}'$
200	2.71(22.10)	12.44(108.60)	600	9.17	18.80
300	2.67(18.28)	12.39(100.70)	700	8.79	18.30
400	2.60(12.66)	12.31(81.80)	800	8.35	17.70
600	2.42	12.05	900	7.83	17.00
800	2.16	11.56	1000	7.22	16.10

TABLE III. The cross sections for the processes $e^-e^+ \rightarrow F\bar{F}$ (where $F = l', \nu'$) at the collision center-of-mass energy $\sqrt{s} = 1$ TeV.

Cross sections (fb)	Z'_S	Z'_ψ	Z'_χ	Z'_η	Z'_{B-L}
$e^-e^+ \rightarrow l'^-l'^+$	105.17	107.65	99.92	105.50	104.78
$e^-e^+ \rightarrow \nu'\bar{\nu}'$	16.04	25.55	27.03	24.18	24.48

TABLE IV. The cross sections for the process $e^-e^+ \rightarrow F\bar{F}$ (where $F = t', b', l', \nu'$) at $\sqrt{s} = 3$ TeV.

Cross section (fb)	Z'_S	Z'_ψ	Z'_χ	Z'_η	Z'_{B-L}
$e^-e^+ \rightarrow t'\bar{t}'$	84.75	15.72	26.46	45.74	24.14
$e^-e^+ \rightarrow b'\bar{b}'$	95.13	16.16	14.91	7.48	6.84
$e^-e^+ \rightarrow l'^-l'^+$	35.59	15.62	38.51	19.35	21.05
$e^-e^+ \rightarrow \nu'\bar{\nu}'$	49.60	0.93	5.80	3.29	3.16

through Z' effects are shown in Table III for ILC with $\sqrt{s} = 1$ TeV. In Table IV the cross sections for the pair production of t' and b' quarks are presented for CLIC with $\sqrt{s} = 3$ TeV through different Z' models. In Tables III and IV, we assume the Z' boson mass $m_{Z'} = 2500$ GeV.

The leptonic decay mode of the Z' boson has a lower branching ratio than the hadronic one, but the cross section for the process $e^-e^+ \rightarrow l'^-l'^+$ is comparable with the $t'\bar{t}'$ pair production for some Z' models. The intermediate goal after the discovery of the Z' boson and the fourth-family fermions would be to understand their properties and couplings. The forward-backward asymmetry and the invariant mass spectrum of the heavy fermions could help to identify the nature of these new particles.

IV. FORWARD-BACKWARD ASYMMETRY

The forward-backward asymmetry A_{FB} is defined as the relative difference between the cross sections with $\cos\theta > 0$ and $\cos\theta < 0$, with θ being the angle between the heavy fermion F and the initial electron in the center-of-mass frame:

$$A_{FB} = \frac{\sigma(\cos\theta > 0) - \sigma(\cos\theta < 0)}{\sigma(\cos\theta > 0) + \sigma(\cos\theta < 0)}.$$

Since the photon has only vector-like couplings to charged fermions the photon exchange cannot generate an asymmetry; however, the Z and Z' bosons exchange, and their interference can generate an asymmetry for the fourth-family fermions. If the heavy fermions are localized differently along a new dynamical symmetry breaking, one can then expect that the interactions of heavy fermions can be different from those of the light fermions. The presence of the s -channel resonance in $F\bar{F}$ production could be identified by an examination of the invariant mass distributions with sufficient statistics. It is seen from Fig. 3 that the asymmetry changes sign at a value of $M_{Z'}$ near the center-of-mass energy. At relatively low $M_{Z'}$ the asymmetry value is around 0.6 (0.4) for t' (b') pair production, with the contribution of the sequential Z' boson at a center-of-mass energy of 3 TeV. However, it has a value around 0.3 (0.45) for the large $M_{Z'}$ region. Figures 4 and 5 show the asymmetries for the fourth-family leptons depending on the Z' mass. Concerning the other Z' models, different asymmetry behaviors of the fourth-family fermions can be seen in Figs. 3–5, depending on the mass of Z' boson.

In order to see how the asymmetry changes depending on the heavy fermion mass M_F we plot Fig. 6 without the Z' contribution. One may comment that the asymmetry A_{FB} for l' pair production is higher than that of ν' at ILC and CLIC energies. As can be seen from the differential cross section in the Appendix, fourth-family fermions have different vector and axial couplings to the Z boson. This can generate different asymmetries for the pair production of fourth-family fermions at linear colliders. Pairs of heavy charged fermions can couple to photons and Z bosons and interfere with each other, while the heavy neutrino pair can couple to Z bosons; therefore, we expect a lower asymmetry for the neutrinos in the SM framework. Considering the current mass limits for $m_{b'}$ and $m_{t'}$ the asymmetry is given for the CLIC energy. For the forward-backward asymmetry of the fourth-family fermions depending on the invariant

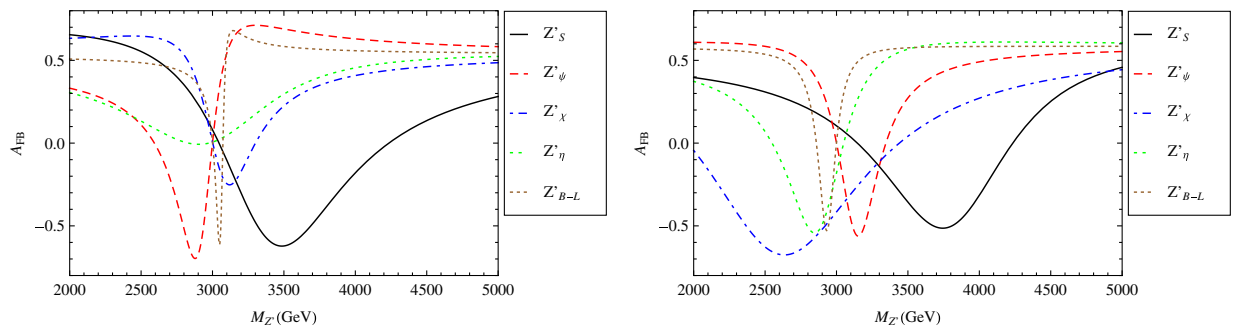


FIG. 3 (color online). Forward-backward asymmetry for t' (left) and b' (right) production within different Z' models at a center-of-mass energy of 3 TeV.

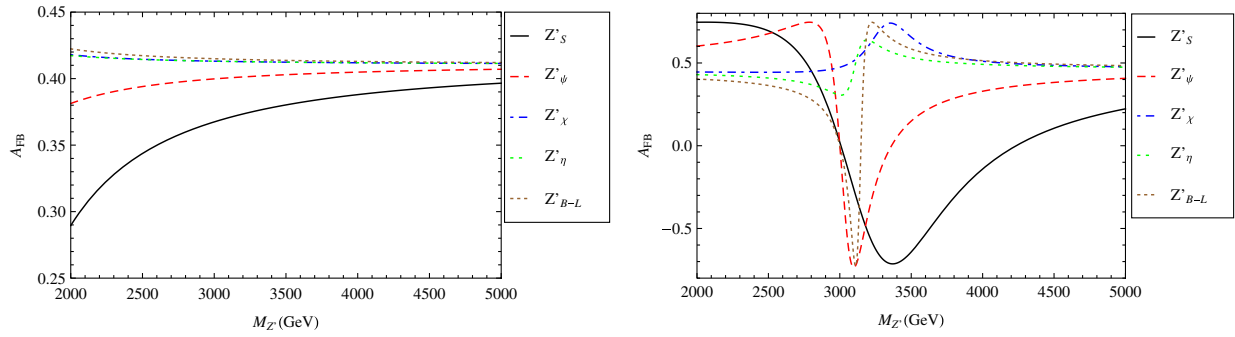


FIG. 4 (color online). Forward-backward asymmetry for the l' lepton within different Z' models at the center-of-mass energies 1 TeV (left) and 3 TeV (right).

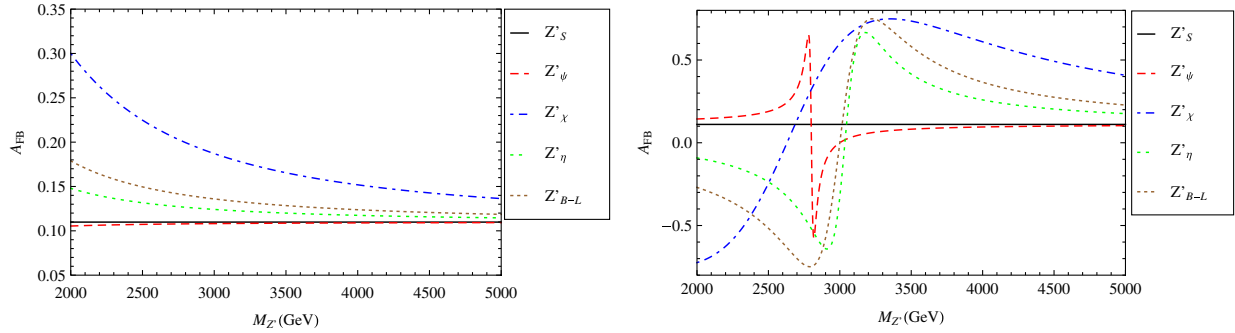


FIG. 5 (color online). The same as Fig. 4, but for $\nu l'$.

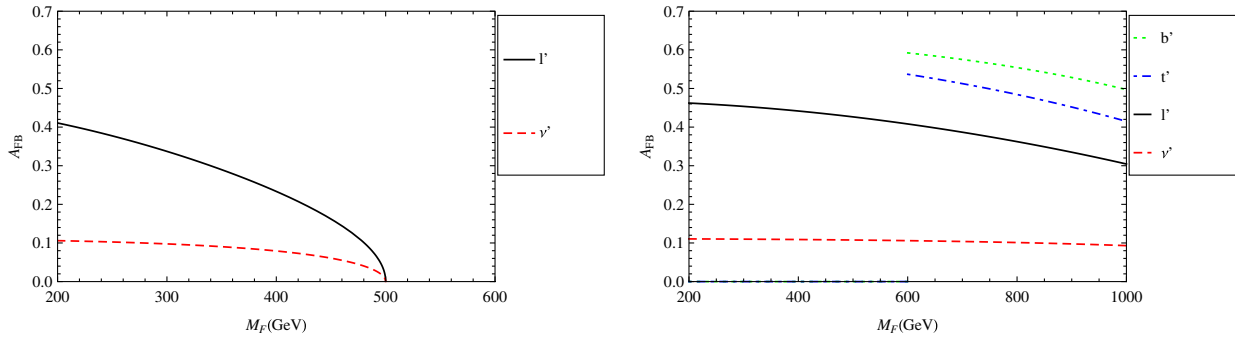


FIG. 6 (color online). The forward-backward asymmetries for fourth-family leptons (l' , $\nu l'$) at $\sqrt{s} = 1$ TeV (left) and for fourth-family fermions (t' , b' , l' , $\nu l'$) at $\sqrt{s} = 3$ TeV (right) depending on their masses.

mass ($M_{F\bar{F}}$), the initial-state radiation (ISR), and beamstrahlung (BS) effects, we use CalcHEP [30] with the beam parameters for the ILC [26] and CLIC [28], as presented in Table V.

TABLE V. The collider beam parameters of the ILC and CLIC needed to calculate the ISR and BS.

	ILC (1 TeV)	CLIC (3 TeV)
Horizontal beam size (nm)	640	45
Vertical beam size (nm)	5.7	1
Bunch length (mm)	0.3	0.044
Number of particles in the bunch (N)	2×10^{10}	3.72×10^9
Design luminosity ($\text{cm}^{-2} \text{s}^{-1}$)	2×10^{34}	5.9×10^{34}

The asymmetries (A'_{FB}) defined in terms of differential cross sections are presented in Fig. 7 depending on the invariant mass of heavy fermions for $M_{Z'} = 3500$ GeV at CLIC with $\sqrt{s} = 3$ TeV. For the sequential Z' model, one obtains an asymmetry of 0.3 around $M_{b'\bar{b}'} = 2000$ GeV at CLIC. One may compare the distributions between the sequential Z' model and the Z'_ψ model. It is seen that the Z'_ψ model generates more asymmetry for charged fermions depending on the invariant mass $M_{F\bar{F}}$. One should note that there is a threshold value for the invariant mass distributions of each type of fermion. These thresholds depend on the value of the heavy-fermion mass. The asymmetry for the neutrino remains approximately at the same level for the interested mass region within these Z' models.

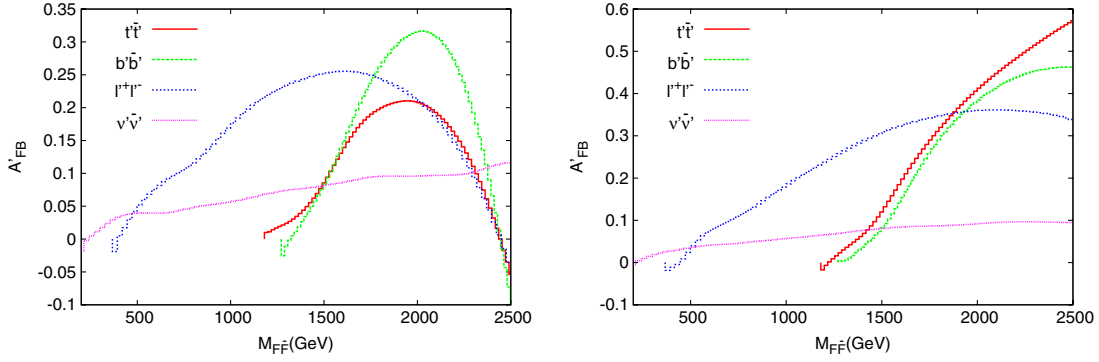


FIG. 7 (color online). Asymmetry depending on the heavy-fermion invariant mass for the sequential Z'_S model (left) and the Z'_ψ model (right) for $m_{Z'} = 3500$ GeV at CLIC with $\sqrt{s} = 3$ TeV.

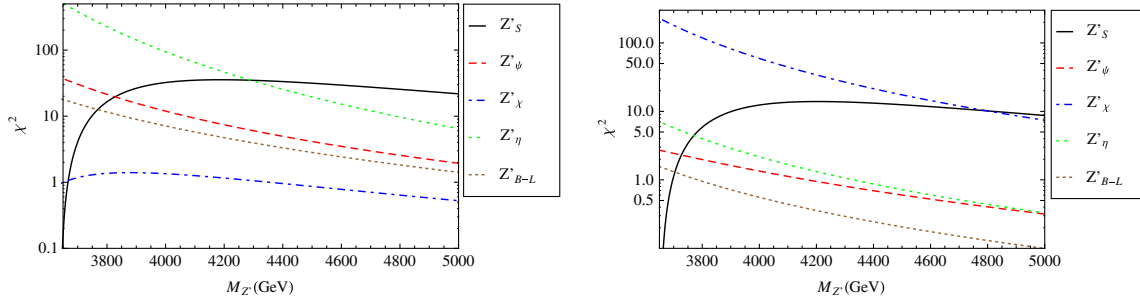


FIG. 8 (color online). The χ^2 distribution for the t' (left) and b' (right) pair production processes depending on the Z' mass at $\sqrt{s} = 3$ TeV.

V. ANALYSIS

In order to analyze the Z' models we define a χ^2 function, given by

$$\chi^2 = \frac{(\sigma^{\text{with } Z'} - \sigma^{\text{no } Z'})^2}{\sigma^{\text{no } Z'} / (\text{BR}\epsilon L_{\text{int}})},$$

where $\sigma^{\text{with } Z'}$ and $\sigma^{\text{no } Z'}$ are the cross sections for pair production of the fourth-family fermions with a Z' boson and without a Z' boson, respectively. The integrated luminosity L_{int} is taken as 200 fb^{-1} at the center-of-mass energy $\sqrt{s} = 1$ TeV for ILC and 600 fb^{-1} at $\sqrt{s} = 3$ TeV for CLIC. The BR and ϵ correspond to the branching ratio and efficiency for the considered decay mode, respectively.

First, we take into account the pair production of fourth-family quarks (t' and b') and their decays via $t'\bar{t}' \rightarrow W^+ b W^- \bar{b}$ and $b'\bar{b}' \rightarrow W^- t W^+ \bar{t} \rightarrow W^- W^+ b W^+ W^- \bar{b}$,

respectively. For the t' pair production process, we consider the leptonic decay of one W boson and the hadronic decay of the other W boson, giving the signal $l^\pm + 2b_{\text{jet}} + 2j + \text{MET}$. In Fig. 8, we plot the χ^2 distribution versus $M_{Z'}$ assuming the mass value $m_{t'} = 600$ GeV and the fourth-family Cabibbo-Kobayashi-Maskawa elements $|V_{t'b'}| = 0.993$, $|V_{t'b}| = 0.115$, $|V_{t's}| = 0.034$, $|V_{t'd}| = 0.006$, $|V_{tb'}| = 0.115$, $|V_{cb'}| = 0.034$, and $|V_{ub'}| = 0.014$ [31] at the linear collider center-of-mass energy $\sqrt{s} = 3$ TeV. For b' pair production, we take into account the fact that same-sign W bosons decay leptonically, while the others decay hadronically, leading to the signal $2l^\pm + 2b_{\text{jet}} + 4j + \text{MET}$.

For t' (b') pair production we can identify the Z'_S model in the mass range $m_{Z'} = 3700\text{--}5000$ GeV at a linear collider energy of $\sqrt{s} = 3$ TeV. However, the other models can be identified in the smaller mass range, well above the

TABLE VI. Number of signal (l' and ν' pairs) and background events for relevant final states at $\sqrt{s} = 1$ TeV and $L_{\text{int}} = 200 \text{ fb}^{-1}$. The numbers in the parentheses denote corresponding signal significances.

Signal	Z'_S	Z'_ψ	Z'_χ	Z'_η	Z'_{B-L}	Background
$l'\bar{l}' \rightarrow 2\mu^- + 3\mu^+ + 2j + \text{MET}$	15.6(110.31)	15.9(112.85)	14.8(104.79)	15.6(110.59)	15.5(109.88)	ZZW^+W^- 0.02
$\nu'\bar{\nu}' \rightarrow 2\mu^- + 4j$	151.9(159.29)	241.9(253.66)	255.9(268.29)	229.0(240.09)	231.8(243.00)	$W^+W^-W^+W^-$ 0.91

TABLE VII. The number of signal (t' , b' , l' , and ν' pairs) and background events for $\sqrt{s} = 3$ TeV and $L_{\text{int}} = 600 \text{ fb}^{-1}$. The numbers in the parentheses denote the significances.

Signal	Z'_S	Z'_ψ	Z'_χ	Z'_η	Z'_{B-L}	Background
$t'\bar{t}' \rightarrow l^+ + 2b_j + 2j + \text{MET}$	1582.8(62.15)	293.6(11.53)	494.2(19.41)	854.3(33.55)	450.8(17.70)	$W^+ b W^- \bar{b}$ 648.5
$b'\bar{b}' \rightarrow 2l^+ + 2b_j + 4j + \text{MET}$	206.0(193.82)	34.9(32.92)	32.3(30.39)	16.2(15.23)	14.8(13.93)	$W^- t W^+ \bar{t}$ 1.13
$l'\bar{l}' \rightarrow 2\mu^- + 3\mu^+ + 2j + \text{MET}$	15.6(44.95)	6.8(19.72)	16.9(48.64)	8.5(24.45)	9.2(26.59)	ZZW^+W^- 0.12
$\nu'\bar{\nu}' \rightarrow 2\mu^- + 4j$	1385.5(624.02)	26.0(11.72)	162.0(72.96)	91.7(41.32)	88.3(39.76)	$W^+W^-W^+W^-$ 4.93

experimental limits. Specifically, for the b' pair production the Z'_χ model will give its signature up to a higher mass value.

Second, we consider the pair production of the fourth-family charged lepton and neutrino (l' and ν') and their decays via $l'\bar{l}' \rightarrow W^- \nu' W^+ \bar{\nu}' \rightarrow W^- \mu^\mp W^\pm W^+ \mu^\mp W^\pm$ and $\nu'\bar{\nu}' \rightarrow W^\pm \mu^\mp W^\pm \mu^\mp$ assuming the Majorana nature of the neutrino, respectively. For l' pair production, we assume that the three same-sign W bosons decay leptonically, while the other decays hadronically, giving the signal $3l^\pm + 2\mu^\mp + 2j + \text{MET}$. The results for this signal are given in Tables VI and VII. However, we also consider the final state $l'\bar{l}' \rightarrow W^- \nu' W^+ \bar{\nu}' \rightarrow 8j + 2\mu^\pm$, which is more convenient for separating Z' models at linear colliders for one year of operation. In Fig. 9, we plot the χ^2 distribution for the $2\mu^\pm + 8j$ signal versus $M_{Z'}$ assuming

the mass value $m_{l'} = 200$ GeV and the fourth-family Pontecorvo-Maki-Nakagawa-Sakata elements $U_{\nu' l'} > 0.996$ and $U_{\nu' l} < 0.092$ [32] at the collider energies $\sqrt{s} = 1$ TeV and 3 TeV. For ν' pair production, we assume that the W bosons decay hadronically, leading to the signal $2\mu^\pm + 4j$. The χ^2 distribution is given in Fig. 10 depending on the $M_{Z'}$, assuming the value $m_{\nu'} = 100$ GeV at the center-of-mass energies $\sqrt{s} = 1$ TeV and 3 TeV.

In the l' pair and ν' pair search we can identify the Z'_χ model in the mass range $2000 < m_{Z'} < 2700$ GeV at $\sqrt{s} = 1$ TeV. A higher center-of-mass energy, $\sqrt{s} = 3$ TeV, expands the accessibility to the range $m_{Z'} = 3700\text{--}5000$ GeV.

The number of signal events for the fourth-family pair production processes at the center-of-mass energies $\sqrt{s} = 1$ TeV and 3 TeV are given in Tables VI and VII,

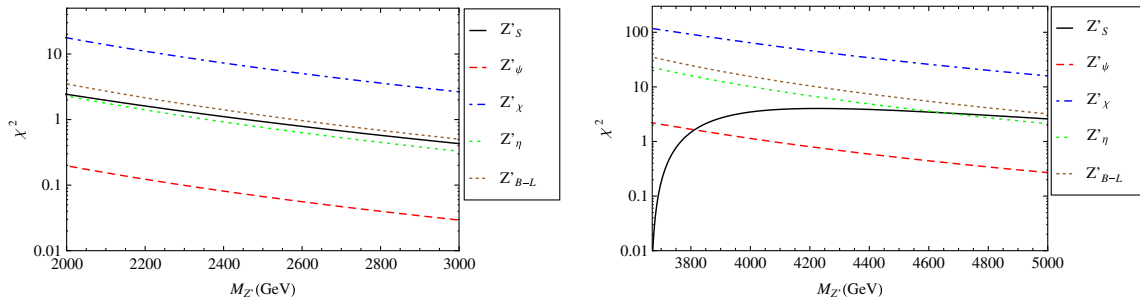


FIG. 9 (color online). The χ^2 distribution for the l' pair production process depending on the Z' mass at $\sqrt{s} = 1$ TeV (left) and $\sqrt{s} = 3$ TeV (right).

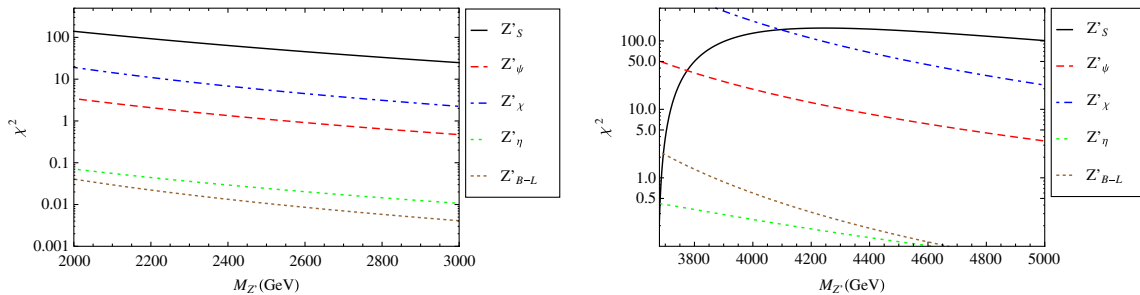


FIG. 10 (color online). The same as Fig. 9, but for the ν' pair production process at $\sqrt{s} = 1$ TeV (left) and $\sqrt{s} = 3$ TeV (right).

respectively. Here, we take the mass of the fourth-family b' quark as $m_{b'} = 650$ GeV and the fourth-family lepton mass as $m_{l'} = 200$ GeV. The corresponding background events are also given in the last column of Tables VI and VII for 200 fb^{-1} and 600 fb^{-1} , respectively. When calculating the number of signal and background events we take into account the corresponding branching ratios and the efficiency factors for the given channel of each signal. In the final state including b quarks, we take the b -tagging efficiency as $\epsilon = 0.5$.

In order to estimate the signal significance for the production of fourth-family fermions we use signal and background events at linear colliders with $\sqrt{s} = 1$ TeV and 3 TeV. As an illustration, considering the $2\mu^- + 3\mu^+ + 2j + \text{MET}$ signal the signal significances (S/\sqrt{B}) in the framework of the Z'_S model are 110.3 (44.95) and 159.3 (624.02) for the l' and ν' pair production processes at 1 (3) TeV, respectively. We will have a larger number of signal events if we choose the channel $2\mu^\pm + 8j$ for the l' pair production. For this channel we expect a rather low background due to at least six gauge bosons in the final state. At the ILC (CLIC), we obtain 460.5 (459.7), 471.4 (201.7), 437.5 (497.5), 461.9 (250.0), and 458.8 (271.8) events for the signal $2\mu^\pm + 8j$ within the Z'_S , Z'_ψ , Z'_χ , Z'_η , and Z'_{B-L} models, respectively. Concerning the fourth-family quarks t' and b' we have the significances 62.15 and 193.82 for the Z'_S model at $\sqrt{s} = 3$ TeV. Providing that the fourth-family fermions exist within the considered mass range, the Z' models can be probed with a large significance at linear colliders.

VI. CONCLUSIONS

We emphasize that exploring the $F\bar{F}$ production cross sections and forward-backward asymmetry at linear colliders will allow further tests of the new models beyond the SM. This work can also be interpreted more generically in the context of any heavy-fermion models, and the fourth-family model can be considered as a template for scenarios of physics beyond the Standard Model.

Taking the masses of the fourth-family fermions as $m_{t'} = 600$ GeV and $m_{b'} = 200$ GeV with the constraints $m_{b'} - m_{t'} = 50$ GeV and $m_{l'} - m_{\nu'} = 100$ GeV, the CLIC (ILC) can produce fourth-family-fermion (t' , b' , l' , and ν') signal events at a rate of 1582, 206, 15 (15), 1385 (151) per year, respectively. We studied the dependence of A_{FB}^F on the heavy-fermion invariant mass $M_{F\bar{F}}$. At CLIC (ILC), the forward-backward asymmetry for t' , b' , l' , and ν' pair production without the Z' contribution can be calculated as 0.55, 0.60, 0.45 (0.40), and 0.10 (0.10) at their mass bounds, respectively. These asymmetries can be affected by the Z' masses in the framework of these models. For an invariant mass of $M_{F\bar{F}} = 2$ TeV, the t' and b' quarks can produce a forward-backward asymmetry of $A_{FB}^F \simeq 0.4$ if the Z'_ψ model is realized. However, heavy-charged-lepton FB asymmetry can also be measured at a relatively low invariant mass range. Performing a χ^2 analysis using the cross sections, we have determined a mass range for the Z' boson that can be accessible at linear collider experiments. It has been shown that through non-resonance observables an e^+e^- collider with energy above the TeV scale has an even higher reach than the LHC for detecting beyond-the-Standard-Model signals [33]. We found that the Z' models give different predictions for the observables and their correlations, and they may be distinguished by jointly studying these observables at linear colliders.

ACKNOWLEDGMENTS

This work is supported in part by the Turkish Atomic Energy Authority (TAEK) under Grant No. CERN-A5.H2.P1.01-10. The work of O.C. and V.C. is supported in part by the State Planning Organization (DPT) under Grant No. DPT2006K-120470.

APPENDIX

The differential cross section for the process $e^+e^- \rightarrow F\bar{F}$ is given by

$$\begin{aligned} \frac{d\sigma(e^-e^+ \rightarrow F\bar{F})}{dt} = & \frac{1}{16\pi s^2} \left\{ \frac{2g_e^4}{s^2} [A_1 Q_F^2] + \frac{g_Z^4}{8[(M_Z^2 - s)^2 + M_Z^2 \Gamma_Z^2]} [(C_A^{e^2} + C_V^{e^2})(C_V^{F^2} A_1 + C_A^{F^2} A_2) + 4C_A^e C_A^F C_V^e C_V^F s A_3] \right. \\ & + \frac{g_{Z'}^4}{8[(M_{Z'}^2 - s)^2 + M_{Z'}^2 \Gamma_{Z'}^2]} [(C_A^{l'e^2} + C_V^{l'e^2})(C_V^{F^2} A_1 + C_A^{F^2} A_2) + 4C_A^{le} C_A^F C_V^{le} C_V^F s A_3] \\ & - \frac{g_e^2 g_Z^2 (-Q_F)(M_Z^2 - s)}{2s[(M_Z^2 - s)^2 + M_Z^2 \Gamma_Z^2]} (C_A^e C_A^F s A_3 + C_V^e C_V^F A_1) - \frac{g_e^2 g_{Z'}^2 (-Q_F)(M_{Z'}^2 - s)}{2s[(M_{Z'}^2 - s)^2 + M_{Z'}^2 \Gamma_{Z'}^2]} (C_A^{le} C_A^F s A_3 + C_V^{le} C_V^F A_1) \\ & + \frac{g_Z^2 g_{Z'}^2 [M_Z^2 (M_{Z'}^2 - s) + M_Z M_{Z'} \Gamma_Z \Gamma_{Z'} + s(s - M_{Z'}^2)]}{[(M_Z^2 - s)^2 + M_Z^2 \Gamma_Z^2][(M_{Z'}^2 - s)^2 + M_{Z'}^2 \Gamma_{Z'}^2]} \{ C_A^e [C_A^{le} (C_A^F C_A^F A_2 + C_V^F C_V^F A_1)] \\ & + C_V^{le} s A_3 (C_A^F C_V^F + C_A^F C_V^F) \} + C_V^e [C_A^F (C_A^{le} C_V^F s A_3 + C_A^{le} C_V^F A_2) + C_V^F (C_A^e C_A^F s A_3 + C_V^{le} C_V^F A_1)] \} \Bigg\}, \end{aligned}$$

where $A_1 = (s+t)^2 + t^2 - 4M_F^2 t + 2M_F^4$, $A_2 = A_1 - 4M_F^2 s$, and $A_3 = s + 2t - 2M_F^2$. g_Z and $g_{Z'}$ are the coupling constants of the neutral-current interactions with the gauge bosons Z and Z' , respectively. C_V^{lF} (C_V^F) and C_A^{lF} (C_A^F) are the vector and axial-vector couplings with the Z' (Z) boson, respectively. s and t are Mandelstam variables. M_Z and $M_{Z'}$ are the masses of the Z and Z' bosons, respectively, and M_F

is the heavy-fermion mass. Γ_Z and $\Gamma_{Z'}$ are decay widths for the Z and Z' bosons, respectively. In order to obtain the differential cross section depending on the scattering angle, $d\sigma/d\cos\theta$, the expression $d\sigma/dt$ should be multiplied by the factor $s\beta/2$, where $\beta = \sqrt{1 - 4M_F^2/s}$, and here we use $t = M_F^2 - s(1 - \beta\cos\theta)/2$.

-
- [1] ATLAS Collaboration, *Phys. Lett. B* **718**, 1284 (2013).
 [2] ATLAS Collaboration, Report No. ATLAS-CONF-2012-130, 2012.
 [3] The CMS Collaboration, *J. High Energy Phys.* **05** (2012) 123.
 [4] CMS Collaboration, *Phys. Lett. B* **718**, 307 (2012).
 [5] G. D. Kribs, T. Plehn, M. Spannowsky, and T. M. P. Tait, *Phys. Rev. D* **76**, 075016 (2007).
 [6] J. Erler and P. Langacker, *Phys. Rev. Lett.* **105**, 031801 (2010).
 [7] ATLAS Collaboration, *Phys. Lett. B* **716**, 1 (2012); CMS Collaboration, *Phys. Lett. B* **716**, 30 (2012).
 [8] The Tevatron New Phenomena and Higgs Working Group for the CDF and D0 Collaborations, [arXiv:1203.3774](https://arxiv.org/abs/1203.3774).
 [9] G. C. Branco, P. M. Ferreira, L. Lavoura, M. N. Rebelo, M. Sher, and J. P. Silva, *Phys. Rep.* **516**, 1 (2012).
 [10] L. Bellantoni, J. Erler, J. J. Heckman, and E. Ramirez-Homs, *Phys. Rev. D* **86**, 034022 (2012).
 [11] J. L. Hewett and T. G. Rizzo, *Phys. Rep.* **183**, 193 (1989).
 [12] A. Leike, *Phys. Rep.* **317**, 143 (1999).
 [13] T. G. Rizzo, [arXiv:hep-ph/0610104](https://arxiv.org/abs/hep-ph/0610104).
 [14] P. Langacker, *Rev. Mod. Phys.* **81**, 1199 (2009).
 [15] CDF Collaboration, *Phys. Rev. Lett.* **106**, 121801 (2011).
 [16] G. Aad *et al.*, *Phys. Rev. Lett.* **107**, 272002 (2011).
 [17] S. Chatrchyan *et al.*, *J. High Energy Phys.* **05** (2011) 093.
 [18] ATLAS Collaboration, *J. High Energy Phys.* **11** (2012) 138.
 [19] CMS Collaboration, *Phys. Lett. B* **714**, 158 (2012).
 [20] V. M. Abazov *et al.* (D0 Collaboration), *Phys. Rev. Lett.* **100**, 142002 (2008).
 [21] CDF Collaboration, *Phys. Rev. D* **83**, 112003 (2011); *Phys. Rev. Lett.* **101**, 202001 (2008).
 [22] The ALEPH Collaboration, The DELPHI Collaboration, The L3 Collaboration, The OPAL Collaboration, The SLD Collaboration, The LEP Electroweak Working Group, The SLD Electroweak and Heavy Flavour Groups, *Phys. Rep.* **427**, 257 (2006).
 [23] A. Djouadi, G. Moreau, and F. Richard, *Nucl. Phys.* **B773**, 43 (2007).
 [24] A. Djouadi, G. Moreau, F. Richard, and R. Singh, *Phys. Rev. D* **82**, 071702 (2010).
 [25] E. L. Berger, Q.-H. Cao, C.-R. Chen, C. Li, and H. Zhang, *Phys. Rev. Lett.* **106**, 201801 (2011).
 [26] J. Brau *et al.*, [arXiv:0712.1950](https://arxiv.org/abs/0712.1950).
 [27] J. Brau *et al.*, [arXiv:0709.1893](https://arxiv.org/abs/0709.1893).
 [28] R. W. Assmann *et al.* (The CLIC Study Team), Report No. CERN 2000-008; Report No. CERN-2003-007; L. Linssen *et al.*, Report No. CERN-2012-003.
 [29] E. Accomando *et al.* (The CLIC Physics Working Group), Report No. CERN-2004-005.
 [30] A. Pukhov *et al.*, [arXiv:hep-ph/9908288](https://arxiv.org/abs/hep-ph/9908288); A. Pukhov, [arXiv:hep-ph/0412191](https://arxiv.org/abs/hep-ph/0412191).
 [31] G. Eilam, B. Melic, and J. Trampetic, *Phys. Rev. D* **80**, 116003 (2009).
 [32] M. A. Schmidt and A. Y. Smirnov, *Nucl. Phys.* **B857**, 1 (2012).
 [33] J. E. Brau *et al.*, [arXiv:1210.0202](https://arxiv.org/abs/1210.0202).